# Fe-N/C catalysts for oxygen reduction based on silicon carbide derived carbon

P.E. Kasatkin[a], R. Jäger[a], E. Härk[a,b,1], P. Teppor[a], I. Tallo[a], U. Joost[c], K. Šmits[d], R. Kanarbik[a], E. Lust[a,*,1]

[a] Institute of Chemistry, University of Tartu, 14a Ravila Str., 50411 Tartu, Estonia
[b] Soft Matter and Functional Materials, Helmholtz Zentrum Berlin, Hahn-Meitner-Platz 1, 14109 Berlin, Germany
[c] Institute of Physics, University of Tartu, 1 W. Ostwaldi Str., 50411 Tartu, Estonia
[d] Institute of Solid State Physics, University of Latvia, Kengaraga 8, 1063 Riga, Latvia

A B S T R A C T

Two different Fe-N/C(SiC) catalysts (Fe + Bipyr/C(SiC) and Fe + Phen/C(SiC)) for oxygen reduction based on silicon carbide derived carbon were synthesized and investigated in 0.1 M KOH aqueous solution by rotating disc electrode method. It was found that the electrocatalytic activity and stability are significantly influenced by the change of the nitrogen ligand in the catalyst. Comparable current density values obtained for 20%Pt-Vulcan electrode could be achieved for Fe + Bipyr/C(SiC) and Fe + Phen/C(SiC) catalysts in alkaline media. The durability tests (~150 h) showed that the decrease of the activity for Fe + Bipyr/C(SiC) and Fe + Phen/C(SiC) is only 0.5 mV $h^{-1}$ and 0.17 mV $h^{-1}$, respectively. The Fe + Bipyr/C(SiC) catalyst demonstrated higher activity in the RDE measurements, but during the long-term test the Fe + Phen/C(SiC) catalyst prove to be more stable than Fe + Bipyr/C(SiC).

## 1. Introduction

Fuel cells have been recognized as promising low temperature energy conversion devices due to their high efficiency and zero/low emission of contaminants [1,2]. Extensive research efforts have been devoted to development of a non-noble oxygen reduction reaction (ORR) catalysts, in order to cut down the cost of fuel cells [3–10]. The most active of these catalysts appear to be the Fe and Co complexes with nitrogen containing macrocycles, such as porphyrins, phthalocyanines and their derivates [7–9]. It has been shown that pyrolysis of other Fe- and Co-complexes with various N-donor ligands, supported on different types of carbons, result in improvement of their activity and stability [1,2,7–13]. Two most common conceptions of the matter are that nitrogen functionalities on the surface of the carbon coordinate with metal ions, where ORR occurs, creating similar moieties to Fe-$N_4$ found in heat treated Fe-$N_4$ macrocycles [7–11] and nitrogen atoms inserted into the carbon structure are the actual active sites for ORR [7–12]. There is also a lot of debating which type of N-atoms is responsible for ORR activity, [12]. Thus, incorporating metal ions during the synthesis of the catalyst is generally found to cause higher ORR activity [4,5,13].

The presented paper studies ORR catalysts in basic media prepared by pyrolizing Fe-ion and N-ligand complexes adsorbed on porous carbide derived carbon (CDC). For the N-donor ligand 1,10-phenanthroline [6,9–11] and similar but cheaper 2,2′-bipyridine were used.

## 2. Experimental

### 2.1. Synthesis of micro-mesoporous CDC

Among the other CDCs studied the SiC is the cheapest one, has proven to have a wide region of ideal polarizability, a very good corrosion resistance, and free of residuals after synthesis [14–19]. Silicon Carbide (98.5% purity, 320 grit powder, Alfa Aesar) powder was held in a flow of $Cl_2$ (99.99%, AGA) at fixed temperature (1100 °C) for the reaction between SiC and $Cl_2$. Thereafter, the obtained CDC powder was treated with $H_2$ at 900 °C for 1.5 h to thoroughly dechlorinate and to remove all possible functional groups from the CDC surface. The CDC powder was further activated with $CO_2$ for 3 h at 950 °C [14–16]. Resulting carbon is noted as C(SiC) in the text.

* Corresponding author.
*E-mail address:* Enn.Lust@ut.ee (E. Lust).
[1] ISE member.

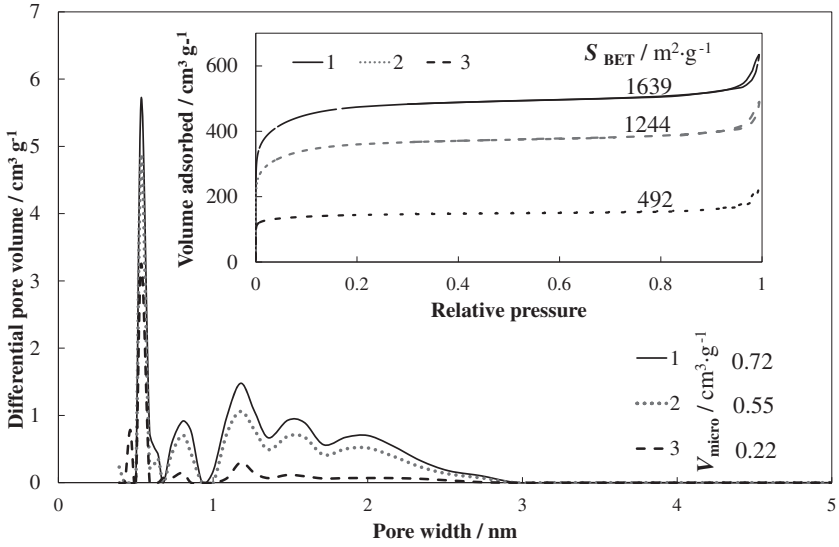


**Fig. 1.** Differential pore volume vs. pore width plots and low-temperature nitrogen adsorption/desorption isotherms (inset) for various catalysts 1 – C(SiC); 2 – Fe + Bipyr/C(SiC); 3 – Fe + Phen/C(SiC).

### 2.2. Catalysts preparation

Fe-N/C(SiC) catalysts were prepared following similar synthesis method reported in the literature [3,5,20–27]. 47 mg $FeSO_4 \cdot 7H_2O$ and 100 mg 1,10-phenanthroline (Phen, ≥ 99%, Aldrich) or 80 mg 2,2′-bipyridine (Bipyr, ReagentPlus®, ≥ 99%, Sigma-Aldrich) were dissolved in 5 ml Milli-$Q^+$ water, mixed and stirred at room temperature (~22 °C) for 1 h to ensure the formation of Fe-ion and N-ligand complexes. The molar ratio of $Fe^{2+}$ ions to N-ligand was 1:3 for both cases [5,20]. Thereafter 100 mg C(SiC) powder was added to the solution together with 10 ml Milli-$Q^+$ water. The resulting mixture was stirred for 2 h for allowing the complexes to adsorb into/onto the carbon support. After that, the slurry was dried by rotatory evaporator and pyrolyzed in the stream of argon (99,999%, AGA) at 800 °C for 1.5 h. Prepared catalysts were noted as Fe + Phen/C(SiC) and Fe + Bipyr/C(SiC). 20%Pt-VulcanXC72® (Fuel Cell Earth) catalyst was studied for comparison.

### 2.3. Preparation of electrodes

The catalyst powder was mixed with Milli-$Q^+$ water, 20 wt% solution of isopropanol (Sigma-Aldrich, > 99%) and Nafion® dispersion (Aldrich). The mixture was sonicated in an ultrasonic bath for 1 h. Thereafter 9 µl of the catalyst ink was pipetted onto the polished glassy carbon disc electrode (Pine Instrument Company, S = 0.196 $cm^2$) to yield the loading of 0.1 $mg_{Fe}\ cm^{-2}$ and dried at ~22 °C [17,18,28].

### 2.4. Electrochemical measurements

All electrochemical measurements were performed using rotating disc electrode (RDE) system (Gamry Instruments Inc., Reference 600) to study ORR kinetics on catalysts prepared. For all experiments a three-electrode electrochemical cell filled with 0.1 M KOH aqueous solution was used. Pt wire mesh ($S_{Pt}$ > 50 $cm^2$) as a counter electrode immersed in the electrolyte solution was separated from the main compartment with the fine membrane and Hg|HgO|0.1 M KOH (denoted as Hg|HgO) was a reference electrode. The RDE data were collected by recording voltammograms at different rotation speeds from 0 to 3000 rev $min^{-1}$ (the potential scan rate was fixed at 10 mV $s^{-1}$) in both Ar and $O_2$ saturated 0.1 M KOH aqueous solutions. Electrochemical impedance spectroscopy was used to measure the electrolyte resistance ($R_s$ ~ 37 Ω at *ac* $f \rightarrow \infty$) of the systems studied and thereafter used to correct the measured potentials against the ohmic potential values. [17,18,28].

### 2.5. Physical characterization methods

Prepared catalysts were characterized by the nitrogen sorption method. ASAP2020 system (Micromeritics) was used for all $N_2$ sorption experiments. The transmission electron microscopy (TEM, Tecnai G20, FEI instrument operating at the 200 kV accelerating voltage) and scanning electron microscopy (SEM, Zeiss EVO MA15, equipped with Oxford X-Max 80 $mm^2$ energy dispersive X-ray spectrometer (EDS)) were used for imaging of the synthesized catalysts. To estimate an overall atomic concentration of different compounds and elements in the catalysts, the X-ray photoelectron spectra (XPS) were conducted in ultra-high vacuum condition using a surface station equipped with an electron energy analyser (SCIENTA SES 100) and a non-monochromatic twin anode X-ray tube (Thermo XR3E2).

## 3. Results

### 3.1. Physical characterization

The specific surface area ($S_{BET}$), the total volume of pores ($V_{tot}$) and the volume of micropores ($V_{micro}$) were calculated using the Brunauer-Emmett-Teller multipoint theory and t-plot method [14–16]. The $S_{BET}$ decreases in the following order: C(SiC) > Fe + Bipyr/C(SiC) > Fe + Phen/C(SiC). In particular, Fe + Phen/C(SiC) has significantly lower $S_{BET}$ value compared to Fe + Bipyr/C(SiC), indicating that during the pyrolysis the iron and 1,10-phenanthroline complex has remarkably changed the catalyst porosity (Fig. 1).

The XPS scanning parameters, and measurement methods, including the average matrix relative sensitivity factor procedure [29], instrument transmission function for data processing and the Casa XPS software [30] used have been described in detail in our previous paper [31]. The XPS spectra of the material surfaces show the presence of carbon, oxygen, iron and nitrogen (Fig. 2, inset Table) and there is no presence of traces of SiC, $SiCl_4$ and $Cl_2$ in catalysts under study. It was found that there are mainly pyridinic and pyrrolic forms of nitrogen in the both catalysts synthesized. However, some quaternary nitrogen and N-O species have been also found. It has been stated by several authors that pyridinic (and pyrrolic) form of the nitrogen plays a very important role as an active center for ORR [6–11].

The SEM images of the Fe-N/C(SiC) catalysts demonstrate the macroscopically porous surfaces (Fig. 3a,c). The EDS analysis show

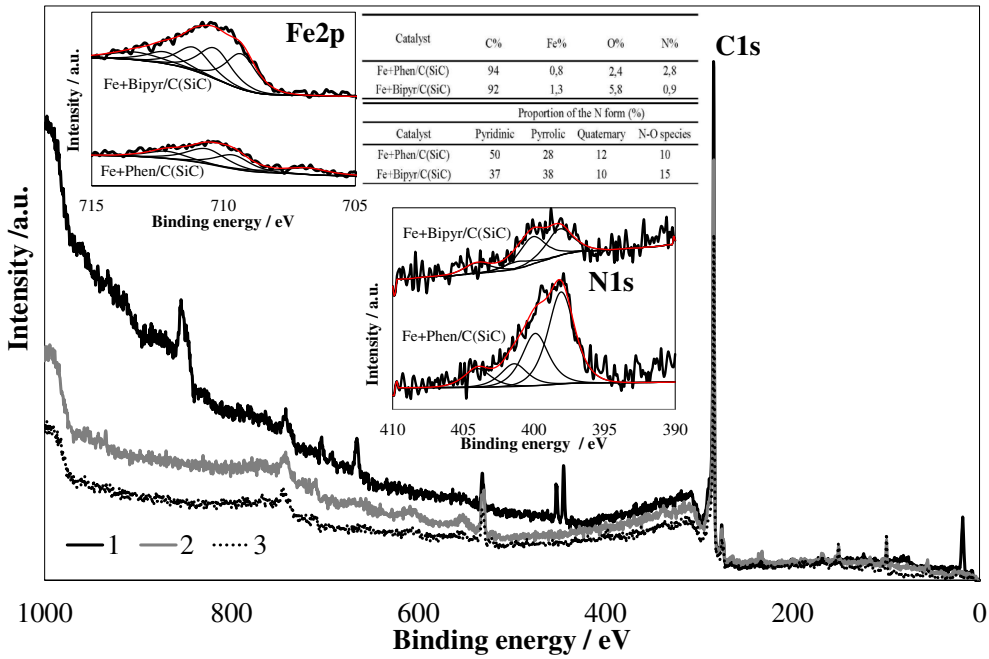


| Catalyst | C% | Fe% | O% | N% |
|---|---|---|---|---|
| Fe+Phen/C(SiC) | 94 | 0,8 | 2,4 | 2,8 |
| Fe+Bipyr/C(SiC) | 92 | 1,3 | 5,8 | 0,9 |

| Catalyst | Proportion of the N form (%) | | | |
|---|---|---|---|---|
| | Pyridinic | Pyrrolic | Quaternary | N-O species |
| Fe+Phen/C(SiC) | 50 | 28 | 12 | 10 |
| Fe+Bipyr/C(SiC) | 37 | 38 | 10 | 15 |

**Fig. 2.** The XPS spectra for catalysts: 1 – C(SiC); 2 – Fe + Bipyr/C(SiC) 3 – Fe + Phen/C(SiC); and insets: Fe2p, N1s spectra and results of the analysis in Table.

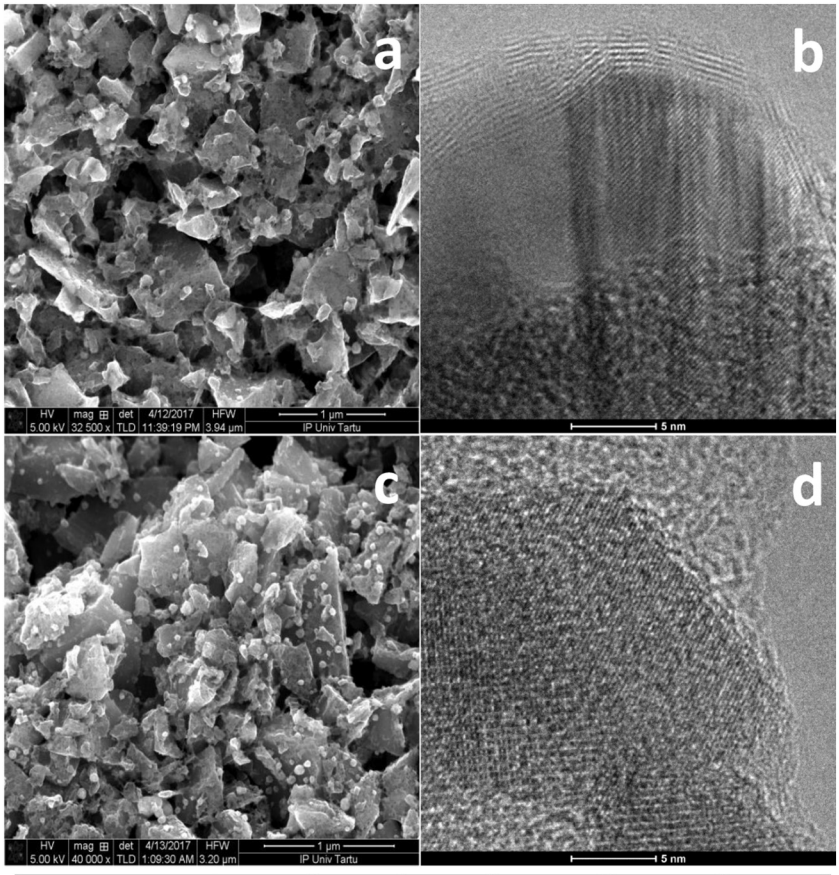


| Element (at%) | C | Fe | O | S | Cu | Total |
|---|---|---|---|---|---|---|
| C(SiC) | 97.67 | - | 2.05 | - | 0.28 | 100.00 |
| Fe+Bipyr/C(SiC) | 87.38 | 1.78 | 10.26 | 0.35 | 0.23 | 100.00 |
| Fe+Phen/C(SiC) | 85.88 | 1.28 | 11.92 | 0.70 | 0.22 | 100.00 |

**Fig. 3.** SEM (a,c) and TEM image (b,d) for catalysts (a,b) Fe + Phen/C(SiC) and (c,d) Fe + Bipyr/C(SiC).

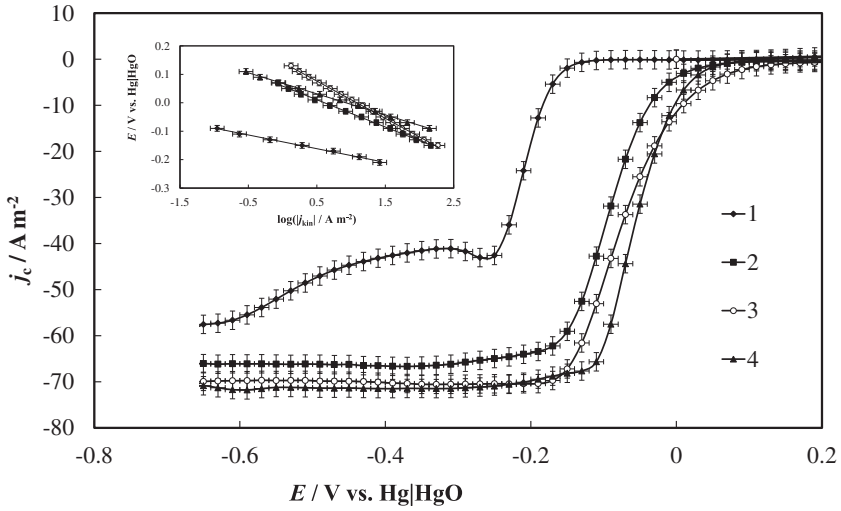


**Fig. 4.** RDE data for ORR in $O_2$ saturated 0.1 M KOH solution at fixed potential scanning rate $\nu = 10$ mV s$^{-1}$ and at electrode rotation rate 3000 rpm$^{-1}$ and inset: Tafel-like plots for catalyst: 1 – C(SiC); 2 – Fe + Phen/C(SiC); 3 – Fe + Bipyr/C(SiC); 4–20%Pt-Vulcan.

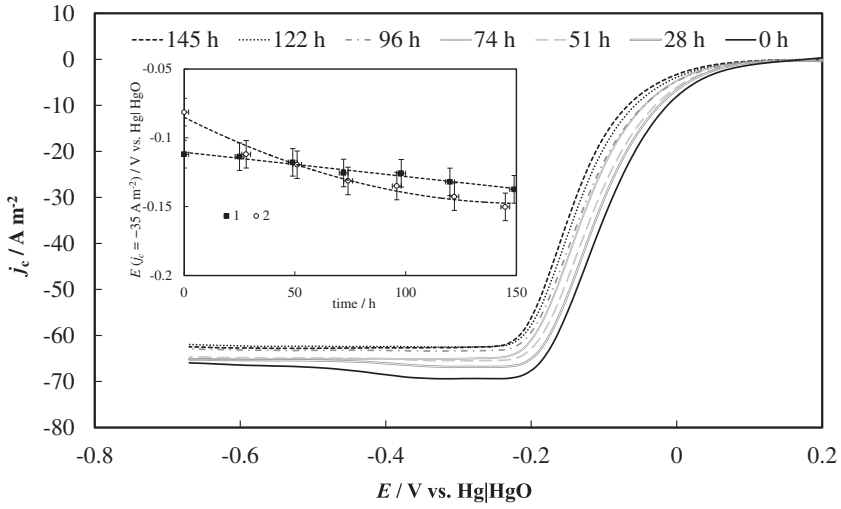


**Fig. 5.** The RDE polarization curves for Fe + Bipyr/C(SiC) 3000 rpm in $O_2$ saturated 0.1 M KOH solution at scan rate of 10 mV s$^{-1}$ recorded after every ~24 h (noted in Figure) and inset: the electrode potential values vs time dependencies at fixed current density ($j_c = -35$ A m$^{-2}$, $\omega = 3000$ rpm, $\nu = 10$ mV s$^{-1}$) value for catalyst: 1 – Fe + Phen/C(SiC); 2 – Fe + Bipyr/C(SiC).

that the amount of the Fe in the catalysts is 1.28 at% or 1.78 at% for Fe + Phen/C(SiC) or Fe + Bipyr/C(SiC), respectively. The finding confirms the XPS data (Table in Fig. 2). A series of TEM images for catalysts (Fig. 3b,d) demonstrate that Fe nanoparticles are surrounded by the amorphous or graphitized areas of the carbon support [32,33].

### 3.2. Electrochemical characterization

RDE current densities measured in $O_2$ saturated solution were corrected with back-ground current densities (Ar saturated solution) and statistically treated, based on five independent experiments to receive the corrected current densities ($j_c$). Fig. 4 shows $j_c$, $E$ curves for all studied catalysts at electrode rotation rate $\omega = 3000$ rpm in $O_2$ saturated 0.1 M KOH solution. Both the Fe + Phen/C(SiC) and Fe + Bipyr/C(SiC) catalysts exhibited noticeably increased activity towards ORR compared to C(SiC). The half-wave potential ($E_{1/2}$) value for Fe + Bipyr/C(SiC) is 20 mV higher than that for the Fe + Phen/C(SiC) catalyst. It should be noted that comparable $E_{1/2}$ values with 20%Pt-Vulcan have been established. Levich plots for Fe-N/C(SiC) catalysts were constructed and the linearity of Levich plots indicates that ORR is limited by mass transport processes within the range of the cathodic electrochemical potentials $E < -0.2$ V vs. Hg|HgO. The calculated number of electrons transferred per one $O_2$ molecule for the Fe + Phen/C(SiC) and Fe + Bipyr/C(SiC) was 3.5 ± 0.1 and 3.8 ± 0.1, respectively, which is in good agreement with literature [1,2,9–12]. For C(SiC) material the number of electrons transferred was 2.5, similar to our previous data for carbide derived carbons [17,18].

Tafel-like plots were constructed and are presented in Fig. 4 inset. The kinetic current density ($j_{kin}$) values used for Tafel-like plots were calculated from Koutecky-Levich equation. The slopes of constructed Tafel-like plots were − 125 and − 96 mV dec$^{-1}$ for Fe + Bipyr/C(SiC) and Fe + Phen/C(SiC), respectively. According to [5,34] the Tafel slope values calculated for the alkaline media may vary within the wide range depending on the type of metal and nitrogen precursors, pyrolysis conditions and the properties of carbon support [35].

Durability tests were conducted for Fe-N/C(SiC) catalysts within ~150 h. The RDE polarization curves in $O_2$ saturated solution were recorded at electrode rotation rates of 1000, 2000 and 3000 rpm, at potential scan rate 10 mV s$^{-1}$, after every ~24 h (Fig. 5). Between the ORR measurements, the electrodes were cycled within the electrode potential range from 0.3 to − 0.7 V vs. Hg|HgO at potential scan rate of 1 mV s$^{-1}$ in Ar saturated 0.1 M KOH. During the durability tests the current densities somewhat decrease within mixed kinetic and diffusion limited current density regions. Inset in Fig. 5 demonstrates the

electrode potential vs time dependencies at fixed current density ($j_c = -35\ A\ m^{-2}$, $\omega = 3000$ rpm, $\nu = 10\ mV\ s^{-1}$) value for both Fe-N/C(SiC) materials. The durability tests showed that the activity slightly decreases in time, being 0.5 mV $h^{-1}$ and 0.17 mV $h^{-1}$ for Fe + Bipyr/C(SiC) and Fe + Phen/C(SiC), respectively. It is interesting to mention that the preliminary RDE test data for Fe + Bipyr/C(SiC) catalyst showed higher activity towards ORR compared to the Fe + Phen/C(SiC) (Fig. 4). However, during the long-term durability test the Fe + Phen/C(SiC) demonstrated a better stability and no further significant decrease of the activity. Therefore, we can conclude that even when the catalyst show higher activity at first, it is not always stable during the long-term test. Thus, the study of the durability and stability of the synthesized catalysts is necessary [35–37].

## 4. Conclusions

For the preparation of the Fe-N/C(SiC) catalyst the $FeSO_4 \cdot 7H_2O$, silicon carbide derived carbon and 1,10-phenanthroline (Phen) or 2,2′-bipyridine (Bipyr) were mixed and thereafter pyrolized at 800 °C. Fe + Phen/C(SiC) and Fe + Bipyr/C(SiC) catalysts have been characterized by the physical and electrochemical methods. It was found that the electrocatalytic activity and stability are significantly influenced by the change of the nitrogen ligand in the catalyst. Comparable current density values obtained with 20%Pt-Vulcan have been achieved for Fe + Bipyr/C(SiC) and Fe + Phen/C(SiC) catalysts in 0.1 M KOH solution. The Fe + Bipyr/C(SiC) showed slightly higher activity towards ORR than Fe + Phen/C(SiC) catalyst. The durability test (~150 h) showed that the ORR activity decreases for Fe + Bipyr/C(SiC) and Fe + Phen/C(SiC) only 0.5 and 0.17 mV $h^{-1}$, respectively, indicating that during the long-term test the Fe + Phen/C(SiC) catalyst was more stable than Fe + Bipyr/C(SiC).

## Acknowledgements

This work was supported by the projects TK141 “Advanced materials and high-technology devices for energy recuperation systems” (2014-2020.4.01.15-0011), NAMUR “Nanomaterials - research and applications” (3.2.0304.12-0397) and by the Estonian Institutional Research Grant No. IUT20-13.

## References

[1] B.C.H. Steele, A. Heinzel, Materials for fuel-cell technologies, Nature 414 (2001) 345–352, http://dx.doi.org/10.1038/35104620.
[2] E. Antolini, Carbon supports for low-temperature fuel cell catalysts, Appl. Catal. B Environ. 88 (2009) 1–24, http://dx.doi.org/10.1016/j.apcatb.2008.09.030.
[3] C.W.B. Bezerra, L. Zhang, K. Lee, H. Liu, A.L.B. Marques, E.P. Marques, H. Wang, J. Zhang, A review of Fe–N/C and Co–N/C catalysts for the oxygen reduction reaction, Electrochim. Acta 53 (2008) 4937–4951, http://dx.doi.org/10.1016/j.electacta.2008.02.012.
[4] G. Wu, A. Santandreu, W. Kellogg, S. Gupta, O. Ogoke, H. Zhang, H.-L. Wang, L. Dai, Carbon nanocomposite catalysts for oxygen reduction and evolution reactions: from nitrogen doping to transition-metal addition, Nano Energy 29 (2016) 83–110, http://dx.doi.org/10.1016/j.nanoen.2015.12.032.
[5] F. Roncaroli, E.S. Dal Molin, F.A. Viva, M.M. Bruno, E.B. Halac, Cobalt and iron complexes with N-heterocyclic ligands as pyrolysis precursors for oxygen reduction catalysts, Electrochim. Acta 174 (2015) 66–77, http://dx.doi.org/10.1016/j.electacta.2015.05.136.
[6] E. Proietti, F. Jaouen, M. Lefèvre, N. Larouche, J. Tian, J. Herranz, J.-P. Dodelet, Iron-based cathode catalyst with enhanced power density in polymer electrolyte membrane fuel cells, Nat. Commun. 2 (2011) 416–424, http://dx.doi.org/10.1038/ncomms1427.
[7] G. Wu, P. Zelenay, Nanostructured nonprecious metal catalysts for oxygen reduction reaction, Acc. Chem. Res. 46 (2013) 1878–1889, http://dx.doi.org/10.1021/ar400011z.
[8] J.-P. Dodelet, Oxygen reduction in PEM fuel cell conditions: heat-treated non-precious metal-N4 macrocycles and beyond, N4-Macrocycl. Met. Complexes, Springer, 2006, pp. 83–147 (http://link.springer.com/chapter/10.1007/978-0-387-28430-9_3 (accessed August 4, 2016)).
[9] U. Tylus, Q. Jia, K. Strickland, N. Ramaswamy, A. Serov, P. Atanassov, S. Mukerjee, Elucidating oxygen reduction active sites in pyrolyzed metal–nitrogen coordinated non-precious-metal electrocatalyst systems, J. Phys. Chem. C. Nanomater. Interfaces. 118 (2014) 8999–9008, http://dx.doi.org/10.1021/jp500781v.
[10] G. Liu, X. Li, P. Ganesan, B.N. Popov, Development of non-precious metal oxygen-reduction catalysts for PEM fuel cells based on N-doped ordered porous carbon, Appl. Catal. B Environ. 93 (2009) 156–165, http://dx.doi.org/10.1016/j.apcatb.2009.09.025.
[11] C. Santoro, A. Serov, R. Gokhale, S. Rojas-Carbonell, L. Stariha, J. Gordon, K. Artyushkova, P. Atanassov, A family of Fe-N-C oxygen reduction electrocatalysts for microbialfuel cell (MFC) application: relationships between surface chemistry and performances, Appl. Catal. B Environ. 205 (2017) 24–33, http://dx.doi.org/10.1016/j.apcatb.2016.12.013.
[12] U.I. Kramm, J. Herranz, N. Larouche, T.M. Arruda, M. Lefèvre, F. Jaouen, P. Bogdanoff, S. Fiechter, I. Abs-Wurmbach, S. Mukerjee, J.-P. Dodelet, Structure of the catalytic sites in Fe/N/C-catalysts for O2-reduction in PEM fuel cells, Phys. Chem. Chem. Phys. 14 (2012) 11673–11688, http://dx.doi.org/10.1039/c2cp41957b.
[13] C. Gumeci, N. Leonard, Y. Liu, S. McKinney, B. Halevi, S.C. Barton, Effect of pyrolysis pressure on activity of Fe–N–C catalysts for oxygen reduction, J. Mater. Chem. A 3 (2015) 21494–21500, http://dx.doi.org/10.1039/c5ta05995j.
[14] E. Tee, I. Tallo, H. Kurig, T. Thomberg, A. Jänes, E. Lust, Huge enhancement of energy storage capacity and power density of supercapacitors based on the carbon dioxide activated microporous SiC-CDC, Electrochim. Acta 161 (2015) 364–370, http://dx.doi.org/10.1016/j.electacta.2015.02.106.
[15] M. Käärik, M. Arulepp, M. Karelson, J. Leis, The effect of graphitization catalyst on the structureand porosity of SiC derived carbons, Carbon 46 (2008) 1579–1587, http://dx.doi.org/10.1016/j.carbon.2008.07.003.
[16] H. Kurig, M. Russina, I. Tallo, M. Siebenbürger, T. Romann, E. Lust, The suitability of infinite slit-shaped pore model to describe the pores in highly porous carbon materials, Carbon 100 (2016) 617–624, http://dx.doi.org/10.1016/j.carbon.2016.01.061.
[17] R. Jäger, P.E. Kasatkin, E. Härk, E. Lust, Oxygen reduction on molybdenum carbide derived micromesoporous carbon electrode in alkaline solution, Electrochem. Commun. 35 (2013) 97–99, http://dx.doi.org/10.1016/j.elecom.2013.08.001.
[18] E. Härk, R. Jäger, I. Tallo, T. Thomberg, H. Kurig, M. Russina, N. Kardjilov, I. Manke, A. Hilger, E. Lust, Different carbide derived nanoporous carbon supports and electroreduction of oxygen, ECS Trans. 66 (24) (2015) 69–80, http://dx.doi.org/10.1149/06624.0069ecst.
[19] V. Presser, M. Heon, Y. Gogotsi, Carbide-derived carbons – from porous networks to nanotubes and graphene, Adv. Funct. Mater. 21 (2011) 810–833, http://dx.doi.org/10.1002/adfm.201002094.
[20] L. Wang, P. Liang, J. Zhang, X. Huang, Activity and stability of pyrolyzed iron ethylenediaminetetraacetic acid as cathode catalyst in microbial fuel cells, Bioresour. Technol. 102 (2011) 5093–5097, http://dx.doi.org/10.1016/j.biortech.2011.01.025.
[21] M. Bron, S. Fiechter, M. Hilgendorff, P. Bogdanoff, Catalysts for oxygen reduction from heat-treated carbon-supported iron phenantroline complexes, J. Appl. Electrochem. 32 (2002) 211–216, http://dx.doi.org/10.1023/A:1014753613345.
[22] R. Kothandaraman, V. Nallathambi, K. Artyushkova, S.C. Barton, Non-precious oxygen reduction catalysts prepared by high-pressure pyrolysis for low-temperature fuel cells, Appl. Catal. B Environ. 92 (2009) 209–216, http://dx.doi.org/10.1016/j.apcatb.2009.07.005.
[23] Y.-L. Liu, X.-Y. Xu, P.-C. Sun, T.-H. Chen, N-doped porous carbon nanosheets with embedded iron carbide nanoparticles for oxygen reduction reaction in acidic media, Int. J. Hydrog. Energy 40 (2015) 4531–4539, http://dx.doi.org/10.1016/j.ijhydene.2015.02.018.
[24] K.C. Heo, K.S. Nahm, S.-H. Lee, P. Kim, Heat-treated 2,2′-bipyridine iron complex supported on polypyrrole-coated carbon for oxygen reduction reaction, J. Ind. Eng. Chem. 17 (2011) 304–309, http://dx.doi.org/10.1016/j.jiec.2011.02.028.
[25] Y. Qiu, L. Gao, Metal-urea complex—a precursor to metal nitrides, J. Am. Ceram. Soc. 87 (2004) 352–357, http://dx.doi.org/10.1111/j.1551-2916.2004.00352.x.
[26] O.B. Ibrahim, M.S. Refat, M. Salman, M.M. AL-Majthoub, Chemical studies on the uses of urea complexes to synthesize compounds having electrical and biological applications, Int. J. Mater. Sci. 2 (2012) 67–82.
[27] M. Saeed-ur-Rehman, S. Ikram, A. Rehman, Shahnawaz Faiz, Synthesis, characterization and antimicrobial studies of transition metal complexes of imidazole derivative, Bull. Chem. Soc. Ethiop. 24 (2010) 201–207, http://dx.doi.org/10.4314/bcse.v24i2.54743.
[28] R. Jäger, E. Härk, P.E. Kasatkin, E. Lust, Investigation of a carbon-supported Pt electrode for oxygen reduction reaction in 0.1 M KOH aqueous solution, J. Electrochem. Soc. 161 (2014) F861–F867, http://dx.doi.org/10.1149/2.0491409jes.
[29] M.P. Seah, I.S. Gilmore, S.J. Spencer, Quantitative XPS: I. analysis of x-ray photoelectron intensities from elemental data in a digital photoelectron database, J. Electron Spectrosc. Relat. Phenom. 120 (2001) 93–111, http://dx.doi.org/10.1016/S0368-2048(01)00311-5.
[30] N. Fairley, CasaXPSversion 2.3.12. www.casaxps.com, (2000).
[31] R. Jäger, E. Härk, T. Romann, U. Joost, E. Lust, C($Mo_2C$) and Pt–C($Mo_2C$) based mixed catalysts for oxygen reduction reaction, J. Electroanal. Chem. 761 (2016) 89–97, http://dx.doi.org/10.1016/j.jelechem.2015.12.018.
[32] K. Strickland, E. Miner, Q. Jia, U. Tylus, N. Ramaswamy, W. Liang, M.-T. Sougrati, F. Jaouen, S. Mukerjee, Highly active oxygen reduction non-platinum group metal electrocatalyst without direct metal–nitrogen coordination, Nat. Commun. 6 (2015) 7343–7351, http://dx.doi.org/10.1038/ncomms8343.
[33] J.A. Varnell, E.C.M. Tse, C.E. Schulz, T.T. Fister, R.T. Haasch, J. Timoshenko, A.I. Frenkel, A.A. Gewirth, Identification of carbon-encapsulated iron nanoparticles as active species in non-precious metal oxygen reduction catalysts, Nat. Commun. 7 (2016) 12582–12590, http://dx.doi.org/10.1038/ncomms12582.
[34] M.H. Robson, A. Serov, K. Artyushkova, P. Atanassov, A mechanistic study of 4-

aminoantipyrine and iron derived non-platinum group metal catalyst on the oxygen reduction reaction, Electrochim. Acta 90 (2013) 656–665, http://dx.doi.org/10.1016/j.electacta.2012.11.025.

[35] A. Sarapuu, L. Samolberg, K. Kreek, M. Koel, L. Matisen, K. Tammeveski, Cobalt and iron-containing nitrogen-doped carbon aerogels as non-precious metal catalysts for electrochemical reduction of oxygen, J. Electroanal. Chem. 746 (2015) 9–17, http://dx.doi.org/10.1016/j.jelechem.2015.03.021.

[36] S. Li, L. Zhang, J. Kim, M. Pan, Z. Shi, J. Zhang, Synthesis of carbon-supported binary FeCo–N non-noble metal electrocatalysts for the oxygen reduction reaction, Electrochim. Acta 55 (2010) 7346–7353, http://dx.doi.org/10.1016/j.electacta.2010.07.020.

[37] X. Li, G. Liu, B.N. Popov, Activity and stability of non-precious metal catalysts for oxygen reduction in acid and alkaline electrolytes, J. Power Sources 195 (2010) 6373–6378, http://dx.doi.org/10.1016/j.jpowsour.2010.04.019.

Institute of Solid State Physics, University of Latvia as the Center of Excellence has received funding from the European Union's Horizon 2020 Framework Programme H2020-WIDESPREAD-01-2016-2017-TeamingPhase2 under grant agreement No. 739508, project CAMART²